STEM CELLS

EMBRYONIC STEM CELLS/INDUCED PLURIPOTENT STEM CELLS

Generation of iPSCs from Genetically Corrected *Brca2* Hypomorphic Cells: Implications in Cell Reprogramming and Stem Cell Therapy

S. NAVARRO,[a,b] V. MOLEIRO,[a,b] F.J. MOLINA-ESTEVEZ,[a,b] M.L. LOZANO,[a,b] R. CHINCHON,[a,b] E. ALMARZA,[a,b] O. QUINTANA-BUSTAMANTE,[a,b] G. MOSTOSLAVSKY,[c] T. MAETZIG,[d] M. GALLA,[d] N. HEINZ,[d] B. SCHIEDLMEIER,[d] Y. TORRES,[e] U. MODLICH,[d] E. SAMPER,[e] P. RÍO,[a,b] J.C. SEGOVIA,[a,b] A. RAYA,[f,g] G. GÜENECHEA,[a,b] J.C. IZPISUA-BELMONTE,[g,h,i] J.A. BUEREN[a]

[a]Hematopoietic Innovative Therapies Division, Centro de Investigaciones Energéticas, Medioambientales y Tecnológicas (CIEMAT), Madrid, Spain; [b]Centro de Investigación Biomédica en Red de Enfermedades Raras (CIBER-ER), Madrid, Spain; [c]Center for Regenerative Medicine, Boston University School of Medicine, Boston, Massachusetts, USA; [d]Institute of Experimental Hematology, Hannover Medical School, Hannover, Germany; [e]NIMGENETICS, Madrid, Spain; [f]Control of Stem Cell Potency Group, Institute for Bioengineering of Catalonia (IBEC) and Institució Catalana de Recerca i Estudis Avançats (ICREA), Barcelona, Spain; [g]Centro de Investigación Biomédica en Red de Bioingeniería, Biomateriales y Nanomedicina (CIBER-BBN), Barcelona, Spain; [h]Center of Regenerative Medicine in Barcelona, Barcelona, Spain; [i]Gene Expression Laboratory, Salk Institute for Biological Studies, La Jolla, California, USA

Correspondence: Juan A. Bueren, Ph.D., Division of Hematopoietic Innovative Therapies, CIEMAT/CIBERER, Avda/Complutense 40, 28040 Madrid, Spain. Telephone: 34–91-346–6518; Fax: 34–91-346–6484; e-mail: juan.bueren@ciemat.es

Received March 9, 2013; accepted for publication September 5, 2013; first published online in STEM CELLS *EXPRESS* October 29, 2013.

1066-5099/2013/$30.00/0

http://dx.doi.org/10.1002/stem.1586

Key Words. Gene therapy • Induced pluripotent stem cells • Hematopoietic stem cells • Bone marrow aplasia • Cellular therapy • Fanconi anemia

ABSTRACT

Fanconi anemia (FA) is a complex genetic disease associated with a defective DNA repair pathway known as the FA pathway. In contrast to many other FA proteins, $BRCA_2$ participates downstream in this pathway and has a critical role in homology-directed recombination (HDR). In our current studies, we have observed an extremely low reprogramming efficiency in cells with a hypomorphic mutation in *Brca2* (*Brca2*$^{\Delta 27/\Delta 27}$), that was associated with increased apoptosis and defective generation of nuclear RAD51 foci during the reprogramming process. Gene complementation facilitated the generation of *Brca2*$^{\Delta 27/\Delta 27}$ induced pluripotent stem cells (iPSCs) with a disease-free FA phenotype. Karyotype analyses and comparative genome hybridization arrays of complemented *Brca2*$^{\Delta 27/\Delta 27}$ iPSCs showed, however, the presence of different genetic alterations in these cells, most of which were not evident in their parental *Brca2*$^{\Delta 27/\Delta 27}$ mouse embryonic fibroblasts. Gene-corrected *Brca2*$^{\Delta 27/\Delta 27}$ iPSCs could be differentiated in vitro toward the hematopoietic lineage, although with a more limited efficacy than WT iPSCs or mouse embryonic stem cells, and did not engraft in irradiated *Brca2*$^{\Delta 27/\Delta 27}$ recipients. Our results are consistent with previous studies proposing that HDR is critical for cell reprogramming and demonstrate that reprogramming defects characteristic of *Brca2* mutant cells can be efficiently overcome by gene complementation. Finally, based on analysis of the phenotype, genetic stability, and hematopoietic differentiation potential of gene-corrected *Brca2*$^{\Delta 27/\Delta 27}$ iPSCs, achievements and limitations in the application of current reprogramming approaches in hematopoietic stem cell therapy are also discussed. STEM CELLS *2014;32:436–446*

INTRODUCTION

Since the laboratory of Shinya Yamanaka demonstrated that mouse fibroblasts can be reprogrammed into induced pluripotent stem cells (iPSCs) through retroviral-mediated transfer of transcription factors, many studies have reproduced these findings using different approaches [1–3]. The generation of iPSCs from animal models and patients suffering from diverse genetic syndromes has also opened new opportunities for basic and translational research, both to understand the events involved in reprogramming and to implement new cell therapies based on the transplantation of iPSC-derived cells [5, 6].

Concerning the molecular processes that participate in the reprogramming process, previous studies have shown that early reprogramming events induce DNA damage, and also that p53-dependent apoptosis and cell senescence constitute barriers for cell reprogramming [7–12]. Additionally, defective reprogramming has been associated to DNA repair defects, due to mutations in signal transducer genes (*Atm* or *53BP1*) [12], nucleotide excision repair genes (*XPC* and *RAD23B*) [13], or Fanconi anemia (FA) genes involved in the upstream FA pathway or the I-D complexes [14–17]. More recently, two papers have been published showing the involvement of genes participating in non homologous end joining [18, 19] and homology-directed recombination (HDR) [17] in cell reprogramming.

The generation and differentiation of gene-corrected disease-specific iPSCs suggested the possibility of using these cells in regenerative medicine. In this respect, different studies have opened new perspectives in the field of gene and cell therapy with reprogrammed cells. Using a mouse model of sickle cell anemia, Hanna et al. showed the possibility of

rescuing the hematopoiesis of affected mice by transplanting iPS-differentiated cells, previously corrected by gene-editing strategies [20]. Thereafter, we showed the feasibility of generating disease-free hematopoietic progenitors from gene-corrected and reprogrammed skin fibroblasts and keratinocytes obtained from FA patients [14]. This proof of concept was of special interest in genetic diseases like FA, with marked hematopoietic stem cell (HSC) defects. In our previous study, cells from FA-A and FA-D2 patients were used for cell reprogramming [14]. Since then, different studies confirmed our observations showing the limited ability of FA cells to be reprogrammed into iPSCs [15–17].

Using FA cells with a hypomorphic mutation in *Brca2* (*Brca2*$^{\Delta 27/\Delta 27}$) [21, 22], which in contrast to many other FA genes is critical for HDR, we have investigated the implications of this mutation in cell reprogramming and evaluated the potential beneficial effect of gene complementation in the generation of disease-free *Brca2*$^{\Delta 27/\Delta 27}$ cells. Finally, the genetic stability and hematopoietic differentiation potential of gene-corrected reprogrammed *Brca2*$^{\Delta 27/\Delta 27}$ iPSC-derived cells were also investigated.

Materials and Methods

Mouse Adult Fibroblasts and Mouse Embryonic Fibroblasts

Brca2$^{\Delta 27\Delta 27}$ mice (FA-D1) [21, 22], *Fanca*$^{-/-}$ mice (FA-A) [23], and control WT littermates were used. All experimental procedures and animal maintenance were carried out according to Spanish and European regulations (Spanish RD 223/88 and OM 13-10-89 of the Ministry of Agriculture, Food and Fisheries; and European convention ETS-123, for the use and protection of vertebrate mammals used in experimentation and other scientific purposes). Mouse adult fibroblasts (MAFs) were obtained from small biopsies from the ears that were digested for 6 hours in 0.25% collagenase diluted in Dulbecco's modified Eagle's medium (DMEM) (BioWhittaker) with 0.5% penicillin/streptomycin (Invitrogen), at 37°C with shaking. Cells were cultured in F25 flasks (Nunc) in DMEM, 10% fetal bovine serum (FBS) with 2 mM Glutamax (Invitrogen), and 1 mM penicillin/streptomycin. Mouse embryonic fibroblasts (MEFs) were extracted from the chorion of 13.5E pregnant females and were dissociated with 0.05% trypsin (Gibco) until complete cell dissociation. Cells were seeded in DMEM supplemented with 10% fetal bovine serum (FBS) (BioWhittaker) and cultured at 37°C, 5% CO_2, 5% O_2 in 145 cm^2 plates (Nunc). At passage 1, MEFs were used for cell reprogramming.

Genetic Correction of *Brca2*$^{\Delta 27/\Delta 27}$ *Cells* with Lentiviral Vectors

A lentiviral vector carrying the *BRCA2* gene under the control of the spleen focus forming virus promoter (SFFV-*BRCA*-LV) was used to complement *Brca2*$^{\Delta 27/\Delta 27}$ fibroblasts as previously described [14, 24, 25]. Lentiviral vector stocks were prepared and titrated as previously described by Raya et al. [14].

Generation of iPSC

For the reprogramming experiments with retroviral vectors, 50,000 MAFs per well were infected with a 1:1:1:1 mix of *Oct4, Sox2, Klf4*, and *c-Myc(T58A)* retroviral supernatants as previously described [1]. For the reprogramming experiments with the polycistronic lentiviral excisable vector (STEMCCA-LV), 25,000 MEFs were transduced every 24 hours at 37°C, 5% CO_2 in 2 cycles of infection. Supernatants were produced as previously described [26]. Four days after transduction, the medium was replaced by mouse embryonic stem cell (ESC) medium: KO-DMEM (Invitrogen) supplemented with 15% fetal bovine serum (FBS) (Gibco), 2 mM Glutamax (Invitrogen), 50 μM 2-β mercaptoethanol (Gibco), 1% non essential amino acids (BioWhittaker), and 1,000 U/ml leukemia inhibitory factor (LIF) (Chemicon) and changed every day. Between days 13 and 16 after transduction with the reprogramming vectors, isolated colonies were individually picked to ensure that expanded iPSC lines were of clonal origin, as previously described [19].

Alkaline Phosphatase, OCT4, NANOG, and SSEA1 Immunostaining

Alkaline Phosphatase (AP) activity was detected on the cell membrane of colonies fixed with 2% paraformaldehyde according to manufacturer instructions (Millipore). For OCT4, NANOG, and SSEA1 immunostaining, colonies were also fixed and then permeabilized by a treatment with 1% bovine serum albumina (BSA), 10% fetal bovine serum (FBS), 0.3 M glycine, and 0.1% Tween 20 diluted in PBS for 1 hour. hOct3/4-FITC (1:20) (R&D, Minneapolis, www.rndsystems.com). SSEA1-PE (1:200) (R&D Systems, Minneapolis, MN, www.rndsystems.com) and Nanog-PE (1:20) (R&D, Minneapolis, MN) antibodies were incubated with diamidino-2-phenylindole (DAPI) (1:500) (Roche) overnight at 4°C. Preparations were mounted with Mowiol (Fluka) for analysis.

Teratoma Formation

One million iPSCs were subcutaneously injected subcutaneously in recipient NOD Cg-*Prkdc*^{scid} *IL2rg*^{tm1Wjl}/SzJ mice (NSG). Paraffin sections of formalin-fixed teratoma specimens were prepared 4–8 weeks after injection and staining was performed for each specimen: alpha fetoprotein (AFP) (Abcam), FoxA2 (Abcam), Branchury (Abcam), α-ASMA (Abcam), Tuj1 (Abcam), and glial fibrillary acidic protein (Abcam).

Quantitative RT-PCR and Transgene Expression

The *BRCA2* relative transgene expression was determined as previously described [25]. Expression of endogenous mouse pluripotency genes was also determined by qRT-PCR by the same method. *Brca2*$^{\Delta 27/\Delta 27}$ MEFs were used as a negative control. Primers used for expression analyses are detailed in Supporting Information Table S1.

Promoter Methylation Analyses

gDNA from 1 × 10^6 iPSCs, mESCs or fibroblasts was subjected to sodium bisulfite treatment followed by bisulfite-specific PCR. For Oct3/4 promoter analyses, a nested PCR was carried out obtaining a 460 bp long product with 15 CpG islands. The primers used for the first and second amplification of Oct3/4 promoter are described in Supporting Information Table S1. In the Nanog promoter analyses, a single PCR was carried out obtaining a product of 366 bp long with 6 CpG islands (see primers used in Supporting Information Table S1). "Hot start" PCR was performed for 35 cycles consisting of denaturation at 95°C for 1 minute, annealing at 56°C for 1 minute, and

extension at 72°C for 1 minute for all primer sets. The products were separated on a 2% agarose gel and cloned in a TOPO vector (TOPO-TA Cloning Kit for Sequencing; Invitrogen) for DNA sequencing.

Excision of the Reprogramming Cassette and Analysis of Proviral Copy Number by RT-PCR

One hundred thousand cells from diploid iPSC selected clones were transduced with an integration-deficient lentiviral vector pLBid-nlsCre-SF LV. After transduction, cells were seeded on irradiated feeder cells (irrMEFs) and individual colonies with ESC-like morphology were isolated. The quantification of proviral copy number per cell was analyzed by qPCR in a Rotor Gene RG-3000 (Corbett Research Products) using primers against Wpre sequence (Supporting Information Table S1). The β-actin housekeeping gene was used to normalize qPCR data, as previously described by Navarro et al. [22]. Amplification was performed using Syber Green amplification kit (Applied Biosystems). The analysis of the viral copy number was performed by absolute quantification as described by Charrier et al. [27], using a standard curve from a mouse cell line harboring 10 copies of a PGK-EGFP Wpre provirus/cell. Clones with no Wpre (woodchuck hepatitis virus posttranscriptional regulatory element) signal detection were considered for further differentiation experiments.

Karyotype and FISH Analyses

To determine structural chromosomal abnormalities, cells were incubated with 10 μg/ml colcemid (Invitrogen) for 4 hours at 37°C after incubation for 2 hours with or without 0.1 μg/ml of diepoxybutane (Sigma), and then treated with 0.56% KCl for 15 minutes at 37°C and fixed in methanol/acetic acid (3:1). Cell suspensions were dropped onto clean slides and air-dried for 24 hours before hybridization. FISH was carried out using a Cy3-labeled LL$(CCCTAA)_3$ PNA telomeric probe and a FITC-labeled LL(ATTCGTTGGAAACGGGA) PNA centromeric probe (Eurogentec). The post-hybridizations washes (3 × 10 minutes; each one) were performed in PBST 0.1% Tween 20 at 60°C and dehydrated in ethanol (70, 90, and 100%; 5 minutes each). Slides were then counterstained and mounted in Vectashield H-1200 mounting medium with diamidino-2-phenylindole (DAPI) (Vector Laboratories, CA). Fluorescence images were acquired with a Nikon 90i microscope (Nikon Instruments, Melville, NY) fitted with a ×100 planfluor 1.3 N/A objective, appropriate filters, and an Hg Intensilight fluorescence unit. Digital images were acquired with Cytovision Genus software (Genetix, Boston, MA). At least 20 metaphases of each cell line and condition were analyzed. Chromosomal aberrations were identified as follows: chromatid or chromosomal breakages: gaps in one or two chromatids whose corresponding centromere was identified or loss of telomere signal in case of terminal breakage; chromosomal fusions: two chromosomes joined without telomere signals at the fusion point with one centromeric signal; dicentrics: chromosomal fusions between two chromosomes joined without telomere signals at the fusion point with two centromeric signals; radials: a structure thought to result from the fusion of the broken arms of nonhomologous chromosomes that can form trirradials or tetrarradials. The percentage of each type of aberration in each cell line and condition was used for statistical analysis. Where indicated, cells were exposed to diepoxibutane (DEB) 0.1 μg/ml 24 hours prior to analysis.

Rad51 and Apoptosis Studies

For Rad51 foci formation, iPSCs were seeded in gelatin-coated slide chambers at a concentration of 50,000 cells per well. Rad51 foci were determined according to that previously described by Rio et al. [25]. Where indicated, cells were treated 24 hours with 40 nM mitomycin C (MMC) (Sigma Aldrich, Sant Louis, MO, http://www.sigmaaldrich.com/). Apoptosis studies were performed by Annexin V and DAPI staining according to manufacturer instructions (BD Pharmingen) and analyzed by flow cytometry.

In Vitro Hematopoietic Differentiation Studies

iPSC and mES J1 cells were first transduced with a retroviral vector *HoxB4.2αGFP-RV* [28]. Embryoid bodies were generated with transduced cells by trypsinizing them with Trypsin/EDTA 0.25% 1× (Gibco, Grand Island, NY, www.lifetechnologies.com). Cells were seeded onto low attachment six-well plates (Corning, Costar) at a final concentration 10^6 cells per milliliter in StemPro34 (Gibco, Grand Island, NY, www.lifetechnologies.com) enriched with nutrient supplement, 200 mg/ml iron-saturated holotransferrin (Sigma Aldrich, Sant Louis, MO, http://www.sigmaaldrich.com/), 0.4 mM monothyoglycerol (Sigma Aldrich, Sant Louis, MO, http://www.sigmaaldrich.com/), 50 mg/ml ascorbic acid (Sigma Aldrich, Sant Louis, MO, http://www.sigmaaldrich.com/), and 4 ng/ml mBMP4 (Peprotech) and cultured at 37°C, 5% CO_2, 21% O_2. After 48 hours of aggregation, half of the medium was replaced by StemPro34 enriched with nutrient supplement and differentiation cytokines at a final concentration of 5 ng/ml mFGF (Peprotech), 5 ng/ml mActivin (R&D Systems, Minneapolis, MN), 5 ng/ml hVEGF, 20 ng/ml hTPO (human trombopoietin) (Peprotech), and 100 ng/ml mSCF (R&D Systems, Minneapolis, MN). Embryoid bodies were maintained 4 more days in this medium. At day 6, the embryoid bodies were collected and dissociated by trypsinization (0.25% trypsin). The resulting cells were counted and seeded at 2×10^5 cells per milliliter in 2 ml over an irradiated OP9 stroma in six-well plates (Nunc, New York, NY). Cocultures were maintained for 14 days in OP9 coculture medium: IMDM (Iscove's Modified Dulbecco's Medium) 20% FBS (Gibco, Grand Island, NY, www.lifetechnologies.com), 2 mM Glutamax (Invitrogen, Grand Island, NY, www.lifetechnologies.com), 2 mM P/S (Invitrogen, Grand Island, NY, www.lifetechnologies.com), 100 ng/ml Flt-3, 100 ng/ml mSCF (R&D, Minneapolis, MN, www.rndsystems.com), 40 ng/ml TPO (Peprotech), and 40 ng/ml VEGF (Peprotech). Every other day, half of the medium was replaced until the final analysis by fluorescence-activated cell sorting (FACS) at day 10. For FACS analysis and cell transplantation studies with iPSCs-differentiated cells, supernatant cells and trypsinized cells attached to the OP9 stroma were mixed together, centrifuged for 7 minutes at 1,000 rpm and then counted with trypan blue (Sigma-Aldrich, Sant Louis, MO, http://www.sigmaaldrich.com/). From one million to 1.5×10^6 cells/mouse were transplanted into $Brca2^{\Delta 27 \Delta 27}$ recipients previously conditioned with a total body irradiation of 5 Gy of x-rays, close to the lethal dose for these animals [25].

Flow Cytometry Analyses

For surface phenotyping of the iPSC colonies, SSEA-1 antibody (R&D, Systems, Minneapolis, MN, www.rndsystems.com) linked to phycoerythrin (PE) fluorochrome was used. To

analyze the phenotype of hematopoietic progenitors the following antibodies were used: anti-cKit (BD Pharmingen, San Jose, CA, www.bdbiosciences.com), anti-Sca1-PE (BD Pharmingen, San Jose, CA, www.bdbiosciences.com), FLk1-PE (BD Pharmingen, San Jose, CA, www.bdbiosciences.com), anti-CD31-PE (BD Pharmingen, San Jose, CA, www.bdbiosciences.com), anti-CD41-PE (BD Pharmingen, San Jose, CA, www.bdbiosciences.com), anti-CD34-biotin (eBioscience), anti-CD45-PE (BD Pharmingen, San Jose, CA, www.bdbiosciences.com), and anti-AA4.1-FITC (BD Pharmingen, San Jose, CA, www.bdbiosciences.com). To assess the engraftment of recipient mice, 100 μl of peripheral blood from transplanted mice was lysed using cold ammonium chloride buffer (0.155 mM NH_4Cl, 0.01 mM $KHCO_3$, 10^{-4} mM EDTA for 10 minutes at RT) and stained with a combination of specific antibodies marking hematopoietic cells expressing lineage differentiation markers (Mac1-PE/GR1-PE, B220-PE, CD3-PE, and Ter119-PE). Gating was done with matched isotype IgG1-PE, -FITC, and -PE-Cy5 control monoclonal antibodies, all from Pharmingen. Cells were washed in PBA (PBS with 0.1% BSA and 0.01% sodium azide), resuspended in phosphate buffered saline + bovine serum albumina (PBA) plus 2 μg/ml propidium iodide, and analyzed using an EPICS ELITE-ESP cytometer (Beckman Coulter, Inc.). Off-line analysis was done with CXP Analysis 2.1 software (Beckman Coulter, Inc.).

Comparative Genomic Hybridization Studies

A whole genome analysis was conducted using a commercial 180k oligonucleotide mouse array-CGH (AMADID 027411, Agilent Technologies, Santa Clara, CA), following manufacturer's protocol 1 [29]. DNA from WT-Balb/c murine MEFs was used as hybridization control. Microarray data were extracted and visualized using Feature Extraction software v10.7 and Agilent Genomic Workbench v5.0 (Agilent Technologies). Copy number altered regions were detected using ADM-2 (set as 6) statistic provided by DNA Analytics, with a minimum number of five consecutive probes. Genomic build UCSC mm8 (NCBI36) was used for the experiment.

Statistical Analysis

Data from all experiments are represented as mean ± SE. To analyze significant differences among the groups we applied the Mann-Whitney *U* nonparametric test (*, $p < 0.05$).

Results

Relevance of *Brca2* in the Reprogramming of Mouse Fibroblasts to iPSCs

In a first set of experiments, we investigated the relevance of two FA proteins placed upstream and downstream in the FA pathway, *Fanca* and *Brca2*, in cell reprogramming. With this objective, fibroblasts from adult *Fanca*$^{-/-}$ and *Brca2*$^{\Delta 27/\Delta 27}$ mice were transduced with four monocistronic retroviral vectors (RVs) carrying *Sox2*, *Oct4*, *Klf4*, and *c-Myc* [1]. An average number of 550 iPSC clones/10^5 cells were generated from WT fibroblasts, while in the case of *Fanca*$^{-/-}$ and *Brca2*$^{\Delta 27/\Delta 27}$ fibroblasts this number was reduced to 45 and 1 iPSC clones/10^5 cells, respectively ($n = 2$), showing the critical role of BRCA2 in cell reprogramming, as compared to Fanca.

To minimize the possibilities that accumulated mutations in adult *Brca2*$^{\Delta 27/\Delta 27}$ fibroblasts were limiting the reprogramming efficacy of these cells, *Brca2*$^{\Delta 27/\Delta 27}$ MEFs were used in the next experiments. Additionally, to understand whether *Brca2* functions were essential for cell reprogramming, *Brca2*$^{\Delta 27/\Delta 27}$ MEFs were subjected to gene complementation with a lentivirale vector carrying BRCA2 (BRCA2-LV) [25] and reprogramming was induced with a polycistronic LV carrying the reprogramming genes (*Oct4*, *Klf4*, *Sox2*, and *c-Myc*; STEMCCA-LV) [26]. Similarly to what we observed in adult *Brca2*$^{\Delta 27/\Delta 27}$ fibroblasts, the reprogramming efficacy of uncorrected *Brca2*$^{\Delta 27/\Delta 27}$ MEFs was extremely inefficient (no stable iPSC clones could be generated with the STEMCCA-LV in three independent attempts). However, gene-complementation of *Brca2*$^{\Delta 27/\Delta 27}$ cells (c*Brca2*$^{\Delta 27/\Delta 27}$ MEFs), either before or simultaneously to cell reprogramming, generated a mean number of 80 and 150 iPSC clones/10^5 cells, respectively (Fig. 1A). Similar results were obtained when adult *Brca2*$^{\Delta 27/\Delta 27}$ fibroblasts were complemented with the *BRCA2*-LV (not shown).

Taking into account that cell reprogramming induces DNA damage [7–12], and given that *Brca2*$^{\Delta 27/\Delta 27}$ lacks a highly conserved Rad51 binding domain [21, 22], in the next set of experiments we investigated the generation of nuclear RAD51

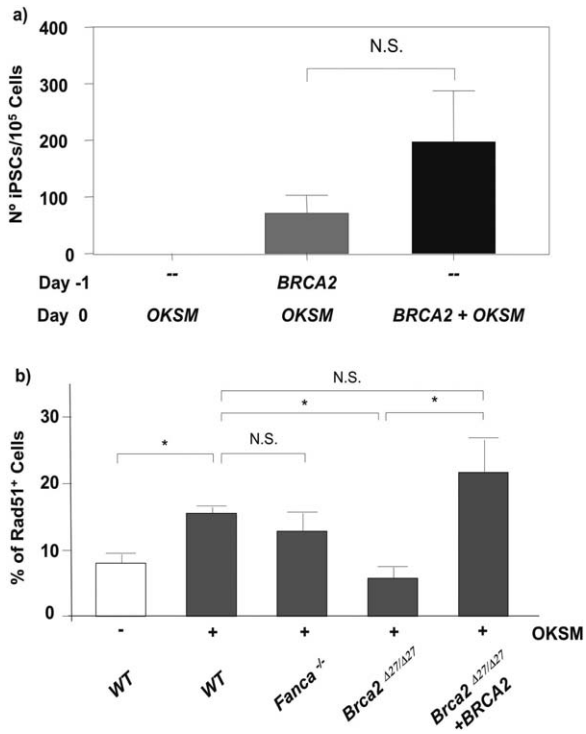

Figure 1. Relevance of *Brca2* on the efficacy of cell reprogramming and the generation of reprogramming-induced nuclear RAD51 foci. **(A):** Comparative numbers of iPSC colonies generated from uncorrected and gene-corrected *Brca2*$^{\Delta 27/\Delta 27}$ mouse embryonic fibroblasts (MEFs). *Brca2*$^{\Delta 27/\Delta 27}$ MEFs were gene-complemented either the day before or simultaneously to transduction with the reprogramming STEMCCA-LV. **(B):** Comparative analysis of the percentage of WT, *Fanca*$^{-/-}$, and *Brca2*$^{\Delta 27/\Delta 27}$ MEFs, either not complemented or complemented with a *BRCA2*-LV (+*BRCA2*), with nuclear RAD51 foci. Analyses were performed 9 days after transduction with STEMCCA-LV (+OKSM), or mock-transduced (−OKSM). In all instances, bars represent means ± SE corresponding to three independent experiments. * Differences were significant at $p < 0.05$. Abbreviation: iPSC, induced pluripotent stem cell.

foci during the reprogramming of WT and *Brca2*$^{\Delta 27/\Delta 27}$ cells (9 days after transduction with the reprogramming LV). As shown in Figure 1B, transduction with the reprogramming vector (+ OKSM, in Fig. 1B) induced a significant increase in the proportion of WT cells with RAD51 foci. A similar proportion of cells with Rad51 foci was observed in reprogrammed *Fanca*$^{-/-}$ MEFs. However, in the case of *Brca2*$^{\Delta 27/\Delta 27}$ MEFs the proportion of cells with RAD51 foci was markedly lower ($p < 0.05$). Significantly, the defective generation of RAD51 foci in *Brca2*$^{\Delta 27/\Delta 27}$ cells during reprogramming was reverted when the genetic defect of these cells was complemented prior to the reprogramming induction (Fig. 1B and Supporting Information Fig. S1).

These results are highly consistent with the recent data from González et al. showing the critical role of *Brca2* and also of *Brca1*—two essential HDR proteins—in cell reprogramming [17], and additionally demonstrate that upon complementation of their genetic defect, reprogramming defects characteristic of *Brca2* mutant cells are efficiently corrected.

To further investigate the consequences of Brca2 mutation during cell reprogramming, the apoptotic response of WT and *Brca2*$^{\Delta 27/\Delta 27}$ to reprogramming induction was determined 9 days after transduction with the reprogramming LV. In order to facilitate the selective analysis of MEFs that were transduced with the reprogramming vector, a STEMCCA-LV version carrying *Oct4*, *Klf4*, *Sox2*, and *mCherry* (OKS/Ch) was used. Figure 2A shows a representative analysis of transduced (Cherry^{+}) WT and *Brca2*$^{\Delta 27/\Delta 27}$ MEFs 9 days after transduction. As shown in Figure 2B, the reprogramming of *Brca2*$^{\Delta 27/\Delta 27}$ cells resulted in a significant increase in the proportion of late apoptotic cells, compared to WT MEFs ($p < .05$). The increased apoptosis rate observed in *Brca2*$^{\Delta 27/\Delta 27}$ cells during cell reprogramming should account, at least in part, for the resistance of these HDR-deficient cells to generate iPSC clones.

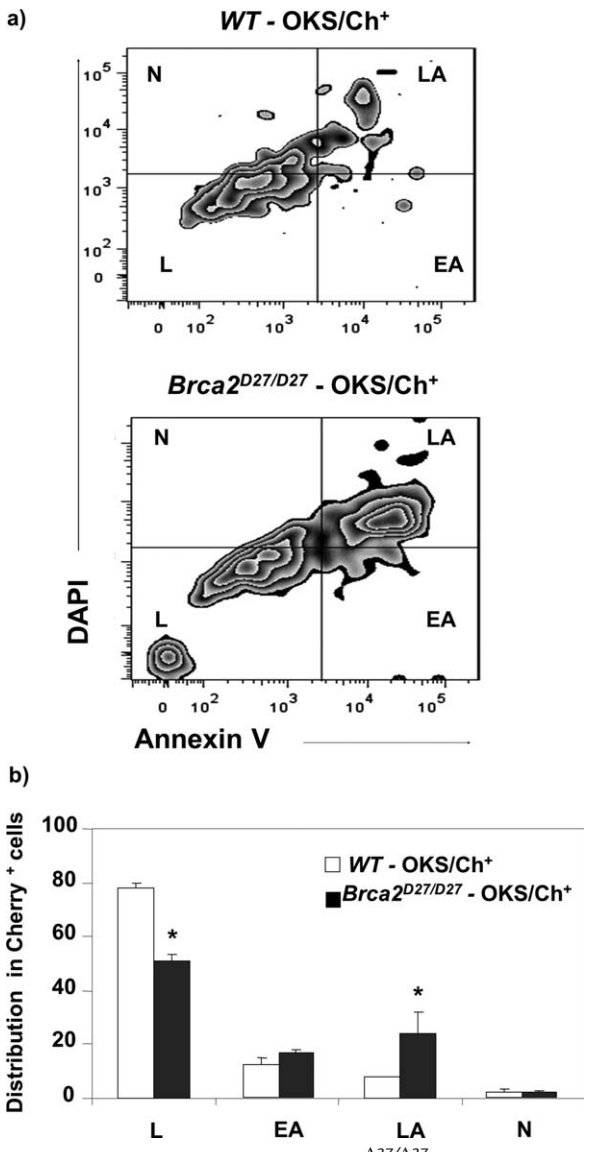

Figure 2. Increased apoptosis in *Brca2*$^{\Delta 27/\Delta 27}$ mouse embryonic fibroblasts (MEFs) during cell reprogramming. **(A):** Representative analysis of alive (L), early apoptotic (EA), late apoptotic (LA), and necrotic (N) WT and *Brca2*$^{\Delta 27/\Delta 27}$ MEFs 9 days after reprogramming. **(B):** Each bar represents the percentage of cells corresponding to the different windows shown in (A). *Differences between WT and *Brca2*$^{\Delta 27/\Delta 27}$ MEFs were significant at $p < .05$. $n = 3$. Abbreviation: DAPI (diamidino-2-phenylindole).

Pluripotency Characterization of Gene-Corrected Brca2$^{\Delta 27/\Delta 27}$ iPSCs

The pluripotent nature of gene-corrected *Brca2*$^{\Delta 27/\Delta 27}$ (c*Brca2*$^{\Delta 27/\Delta 27}$) iPSCs was first determined by AP activity analysis and by the expression of SSEA1 and Nanog. Strong AP staining was observed in all tested clones (Fig. 3A). Similarly, a high proportion of c*Brca2*$^{\Delta 27/\Delta 27}$ iPSCs (around 70%) was positive for SSEA1 by flow cytometry (Fig. 3B, 3C) and expressed medium to high levels of *Nanog* mRNA (Fig. 3D). Despite these observations, c*Brca2*$^{\Delta 27/\Delta 27}$clones in which the reprogramming vector was not excised did not generate teratomas in NSG mice, but rather tumors only containing one of the three germ layers and/or undifferentiated cell masses (Supporting Information Fig. S2A).

The genetic stability of c*Brca2*$^{\Delta 27/\Delta 27}$ iPSCs was investigated by analyzing the ploidy (Fig. 4A) and the karyotype (refer a representative picture in Fig. 4B and individual analyses in Fig. 4C) of 26 out of the 52 iPSC clones that were selected. Analyses performed at passage 17 showed that in the case c*Brca2*$^{\Delta 27/\Delta 27}$, only A12 and A16 iPSCs clones were diploid and had a normal karyotype (Fig. 4C). These clones were then transduced with an integration-deficient Cre-recombinase-LV (pLBid-nlsCre-SF LV) to excise the reprogramming cassette. An evident reduction in the number of STEMCCA copies/cell was observed in all instances. In the case of the A16.Ex10 clone, an average number of 0.3 copies of the reprogramming vector/cell was observed, while in the A16.Ex7 clone no amplification of the reprogramming cassette was observed, indicating that this specific clone was free from the reprogramming vector (Supporting Information Fig. S3).

To investigate the pluripotency of excised iPSCs, further studies were performed with A16.Ex7 and A16.Ex10 c*Brca2*$^{\Delta 27/\Delta 27}$ iPSC clones (data corresponding to A16.Ex7 clone shown in Fig. 5). Immunohistochemical (Fig. 5A) and molecular analyses (Fig. 5B) revealed the complete reprogramming and activation of endogenous pluripotency genes in A16.Ex7 cells (i.e., AP, *Oct3/4*, *SSEA1*, *Nanog*, *c-Myc*, *Klf4*, and *Uft1*). In contrast to the hypermethylation of the *Nanog* and *Oct3/4* promoter observed in parental c*Brca2*$^{\Delta 27/\Delta 27}$ MEFs, both

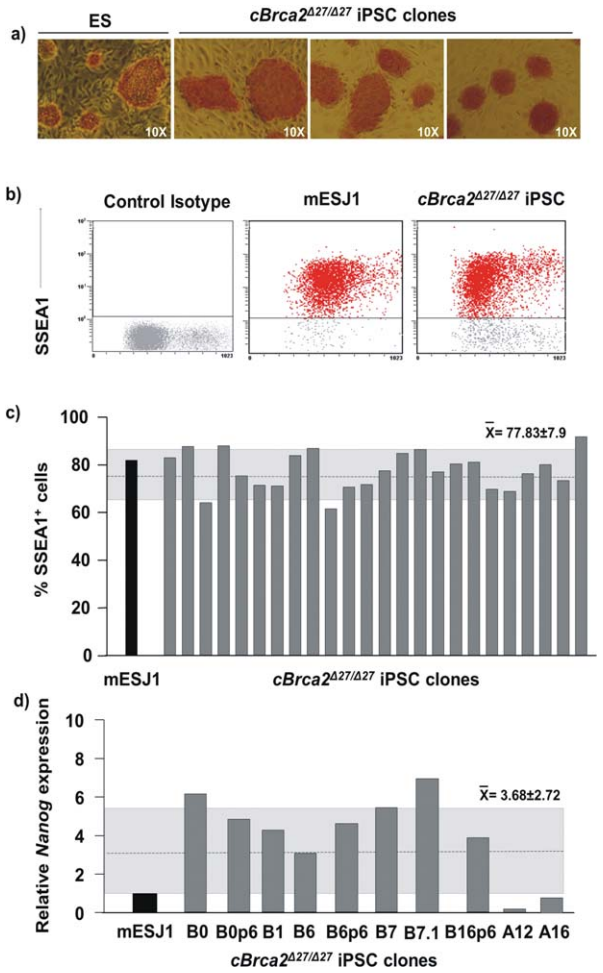

Figure 3. Expression of pluripotency markers in gene-corrected *Brca2*$^{\Delta 27/\Delta 27}$ iPSCs. **(A):** Alkaline phosphatase staining of gene-corrected *Brca2*$^{\Delta 27/\Delta 27}$ iPSC (c*Brca2*$^{\Delta 27/\Delta 27}$ iPSCs) at passage 4. Panels **(B)** and **(C)** show, respectively, representative flow cytometry analysis of SSEA1 expression and individual determinations SSEA1^{+} cells in 24 c*Brca2*$^{\Delta 27/\Delta 27}$ iPSC clones and mESCs (J1). **(D):** Relative *Nanog* expression of 10 c*Brca2*$^{\Delta 27/\Delta 27}$ iPSCs clones compared to the expression determined in mESJ1 cells. Analyses were performed at passages 6–17 (mean and SE values corresponding to all analyzed iPSC clones are shown). Abbreviations: ES, embryonic stem; iPSC, induced pluripotent stem cell.

promoters were hypomethylated in the diploid A16.Ex7 c*Brca2*$^{\Delta 27/\Delta 27}$ iPSC clone (Fig. 5C). Moreover, while no teratomas were generated by non excised cells from this clone, characteristic teratomas containing cells of the three germ layers were observed when excised A16.Ex7 cells were inoculated in NSG mice (Supporting Information Fig. S2B), showing the relevance of the reprogramming cassette excision for the generation of *bona fide* c*Brca2*$^{\Delta 27/\Delta 27}$ iPSCs. When additional karyotype studies of A16.Ex7 and A16.Ex10 clones were performed after three to five passages in culture, we observed that A16-Ex10 clone became hyper-diploid, while A16-Ex7 clone maintained a normal karyotype (Fig. 4C).

Disease-Free Phenotype of Gene-Corrected Brca2$^{\Delta 27/\Delta 27}$ iPSCs

In the next set of experiments, we investigated whether gene-corrected *Brca2*$^{\Delta 27/\Delta 27}$ clones were disease-free. With this aim, we first analyzed the ectopic expression of the *hBRCA2* mRNA conferred by the *BRCA2*-LV used for gene complementation. As shown in Figure 6A, an evident expression of the transgene was observed both in c*Brca2*$^{\Delta 27/\Delta 27}$ MEFs and c*Brca2*$^{\Delta 27/\Delta 27}$ iPSC clones. To confirm the hBRCA2 function in these cells, we investigated the generation of Rad51 foci after DNA damage induced by mitomycin C (MMC) [22, 30] (Fig. 6B). In contrast to the low proportion of Rad51^{+} cells observed in *Brca2*$^{\Delta 27/\Delta 27}$ MEFs, complemented *Brca2*$^{\Delta 27/\Delta 27}$ MEFs and iPSCs evidenced a significant increase in the proportion of Rad51^{+} cells (Fig. 6B and Supporting Information Fig. S4 correspond to A16-Ex7 cells), confirming the functional correction of these cells.

Finally, because FA cells are characterized by their chromosomal instability to DNA cross-linkers, we investigated the generation of chromosomal alterations after DEB-exposure in complemented A16-Ex7 *Brca2*$^{\Delta 27/\Delta 27}$ iPSCs cells as compared to not complemented iPSCs generated after transduction with four reprogramming retroviral vectors (RVs). As shown in Figure 6C, the number of chromosomal breakages, chromosomal fragmentations, and radial fragmentations observed in complemented *Brca2*$^{\Delta 27/\Delta 27}$ iPSCs was significantly lower compared to uncorrected *Brca2*$^{\Delta 27/\Delta 27}$ iPSCs. These results further demonstrate the disease-free condition of *Brca2*$^{\Delta 27/\Delta 27}$ iPSCs generated after gene complementation and cell reprogramming.

Comparative Genomic Hybridization Analyses of Brca2$^{\Delta 27/\Delta 27}$ MEFs and iPSCs

Although A16-Ex7 c*Brca2*$^{\Delta 27/\Delta 27}$ iPSCs had a normal karyotype, we further investigated whether the cell manipulation required for the generation of disease-free and reprogramming vector-free c*Brca2*$^{\Delta 27/\Delta 27}$ iPSCs, induced genetic changes that could be detected by comparative genomic hybridization arrays (aCGH). To this end, DNA samples from A16.Ex7 c*Brca2*$^{\Delta 27/\Delta 27}$ iPSCs and from their parental *Brca2*$^{\Delta 27/\Delta 27}$ MEFs were analyzed, prior to and after gene complementation, relative to WT MEFs that were considered the reference population. As shown in Supporting Information Figure S5A, only a few genetic alterations were observed in uncorrected in vitro expanded *Brca2*$^{\Delta 27/\Delta 27}$ MEFs, which consisted in a duplication at 3qA3 and a deletion at 17qA3.3. After gene correction with the *BRCA2*-lentiviral vector, the same aCGH footprint was observed, indicating that gene correction per se did not induce evident genetic abnormalities in *Brca2*$^{\Delta 27/\Delta 27}$ MEFs. However, additional genetic changes were observed in A16-Ex7 c*Brca2*$^{\Delta 27/\Delta 27}$ iPSCs, including a large duplication covering cytoband 4qD1, 11qB4, 19qA, and a deletion at 13qD1; that were not detected in parental *Brca2*$^{\Delta 27/\Delta 27}$ MEFs (Supporting Information Fig. S5B). The deletion 17qA3.3 observed in parental *Brca2*$^{\Delta 27/\Delta 27}$ MEFs was also present in the iPSCs, confirming the *Brca2*$^{\Delta 27/\Delta 27}$ MEFs origin of these reprogrammed cells. While genetic alterations observed in disease-free c*Brca2*$^{\Delta 27/\Delta 27}$ iPSCs could be related to the HDR-deficient nature of their parental cells, iPSCs generated from the reference WT MEFs also showed a number of genetic alterations (large duplication of cytoband 1qG3qH3, deletion of cytoband 1qH3qH6, and a large duplication of cytoband 12qC3qF2; Supporting Information Fig. S5C), indicating that the *Brca2* mutant background of c*Brca2*$^{\Delta 27/\Delta 27}$ iPSCs should not necessarily account for the genetic changes observed in these reprogrammed cells.

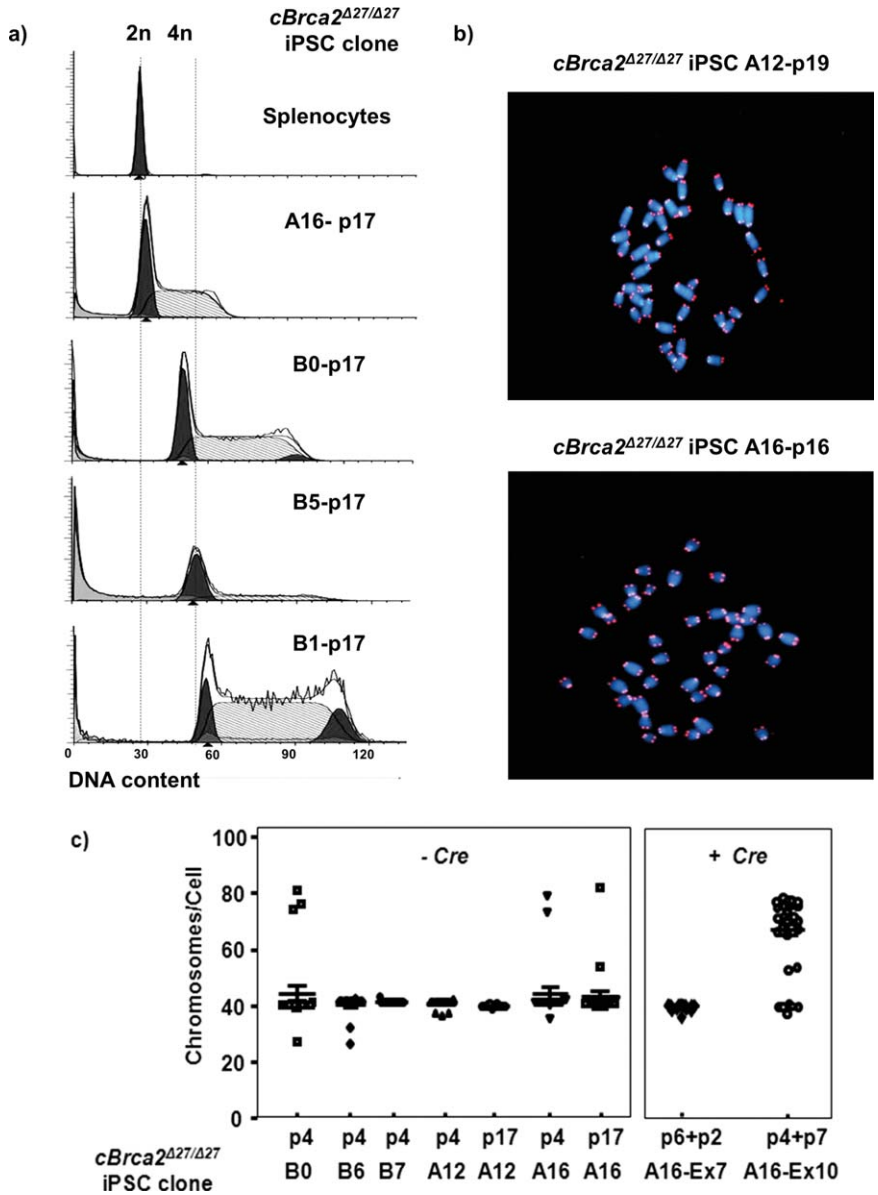

Figure 4. Ploidy and karyotype of gene-corrected *Brca2*$^{\Delta 27/\Delta 27}$ iPSCs. **(A):** Cell cycle histograms illustrating the ploidy of c*Brca2*$^{\Delta 27/\Delta 27}$ iPSCs clones. **(B):** Representative picture showing a normal karyotype in two c*Brca2*$^{\Delta 27/\Delta 27}$ iPSC clones. **(C):** Karyotype analysis of five c*Brca2*$^{\Delta 27/\Delta 27}$ clones (B0-A16) and clones derived from excision of A16 (A16-Ex7 and A16-Ex10). The figure shows individual analyses of chromosome numbers per cell as well as mean and SE values corresponding to each cell type. In unexcised clones, the number of passages at analysis is indicated by the "p" number. In clones where the reprogramming vector was excised, the number of passages prior to and after excision is represented by "p+p." Abbreviation: iPSC, induced pluripotent stem cell.

Hematopoietic Differentiation of Gene-Corrected Brca2$^{\Delta 27/\Delta 27}$ iPSCs

In the final set of experiments, gene-corrected *Brca2*$^{\Delta 27/\Delta 27}$ iPSC clones as well as control mESCs (J1 cell line) and WT iPSCs were differentiated towards the hematopoietic lineage through the generation of embryoid bodies, followed by the coculture of the resulting cells with OP9 stromal cells and transduction with a *HoxB4.2aGFP*-RV [28] (protocol in Supporting Information Fig. S6A). Compared to data obtained with mESCs, the hematopoietic differentiation deduced from the analysis of CD41$^+$, CD34$^+$, CD45$^+$, and c-Kit$^+$ markers was systematically lower in the case of iPSCs, particularly with c*Brca2*$^{\Delta 27/\Delta 27}$ iPSC clones (see representative analyses corresponding to A16Ex7 c*Brca2*$^{\Delta 27/\Delta 27}$ iPSC cells in Supporting Information Fig. S6B, S6C). Neither the use of AM20.1B4 stromal cells nor the differentiation method based on the transduction of iPSC with the *Lhx2* vector [31], improved the differentiation capacity of these cells (not shown). Moreover, although transplantations of mESC-derived hematopoietic cells into irradiated recipients resulted in significant hematopoietic engraftments [32], no reproducible engraftments were observed when A16-Ex7 c*Brca2*$^{\Delta 27/\Delta 27}$ iPSCs were transplanted. In these transplants a reduced number ($<$1%) of Hox-B4/EGFP$^+$ cells, which did not express hematopoietic markers, could be observed for up to 30 days post-transplantation in peripheral blood (PB).

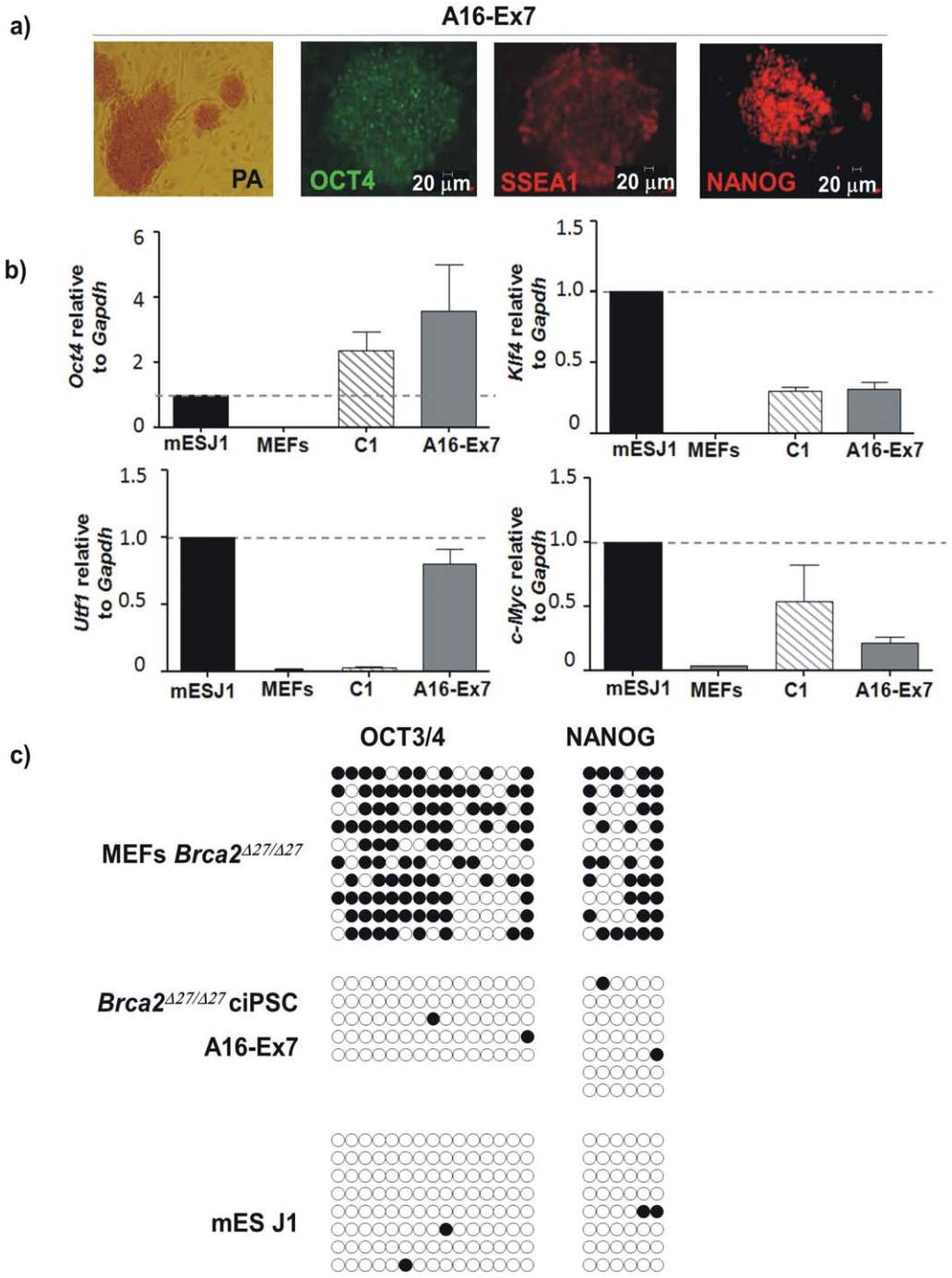

Figure 5. Analysis of pluripotency markers in excised c*Brca2*$^{\Delta 27/\Delta 27}$ induced pluripotent stem cells (iPSCs). **(A):** Representative immunohistochemistry analysis of c*Brca2*$^{\Delta 27/\Delta 27}$ iPSC A16-Ex7 cells with markers characteristic of pluripotent cells. **(B):** RT-PCR analyses of four different transcription factors expressed in primitive cells. **(C):** Methylation status of the *Oct3/4* and *Nanog* promoters in parental *Brca2*$^{\Delta 27/\Delta 27}$ MEFs and in A16-Ex7 c*Brca2*$^{\Delta 27/\Delta 27}$ iPSCs. Abbreviation: MEFs, mouse embryonic fibroblasts.

Discussion

The generation of iPSCs through the ectopic expression of specific transcription factors [1–3] has facilitated the investigation of the molecular insights involved in cell reprogramming [7–16] and opened new possibilities for disease modeling and also for drug development and cell therapy [5, 6].

In the field of FA, significant observations have been achieved thanks to the use of ESCs and the generation of specific iPSC from FA patients and FA mouse models. In our previous study, disease-free hematopoietic progenitors were generated by means of the combined use of gene therapy and cell reprogramming in skin cells from FA-A and FA-D2 patients [14]. Because FA is characterized by a defective content in HSCs in the bone marrow (BM) of these patients [33], our study opened the possibility of generating HSCs from non-hematopoietic tissues in patients with bone marrow failure

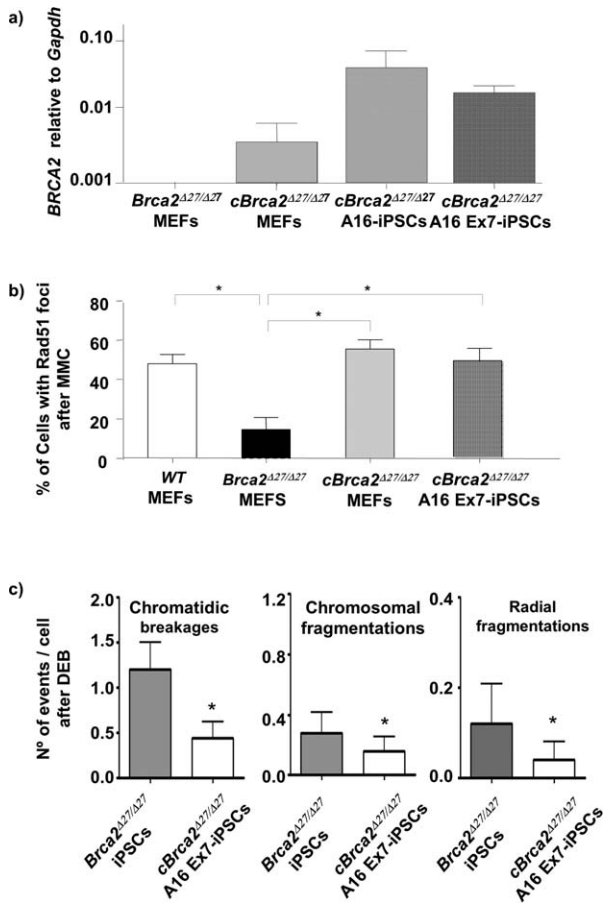

Figure 6. Disease-free phenotype of c*Brca2*$^{\Delta 27/\Delta 27}$ iPSCs. **(A):** Analysis of *hBRCA2* mRNA expression in uncorrected (*Brca2*$^{\Delta 27/\Delta 27}$) and gene complemented (c*Brca2*$^{\Delta 27/\Delta 27}$) MEFs and iPSCs prior to (A16) and after excision (A16Ex7) of the reprogramming vector; $n = 3$. **(B):** Comparative generation of Rad51^{+} cells after MMC exposure of WT and *Brca2*$^{\Delta 27/\Delta 27}$ MEFs and c*Brca2*$^{\Delta 27/\Delta 27}$ MEFs and iPSCs (A16-Ex7); $n = 3$. Fifty cells per group were scored in each analysis. **(C):** Comparative number of chromatidic breakages, chromosomal fragmentations, and radial chromosomes in not complemented (*Brca2*$^{\Delta 27/\Delta 27}$) and complemented (A16 Ex7 c*Brca2*$^{\Delta 27/\Delta 27}$) iPSCs after DEB exposure. Not complemented *Brca2*$^{\Delta 27/\Delta 27}$ iPSCs cells correspond to the clone generated with the four reprogramming RVs. *, $p < .05$; $n = 25$ metaphases were analyzed in each group. iPSCs were analyzed at passages 10–12. Abbreviations: DEB, diepoxibutane; iPSC, induced pluripotent stem cell; MEFs, mouse embryonic fibroblast.

syndromes. By means of the knocking down of *FANCA* and *FANCD2* in hESCs, Tulpule et al. showed that hematopoiesis is impaired in FA from the very early stages of development [34]. Thereafter, Müller et al. showed that cell reprogramming leads to the activation of the FA pathway in response to DNA damage, thus accounting for a decreased reprogramming efficiency in the case of FA cells [15]. Very recently González et al. showed marked reprogramming defects in *Brca1* and *Brca2/Fancd1* mutant cells, and also in cells with a downregulated expression of Rad51 [17].

Our results in Figure 1 showing the extremely low reprogramming efficacy of *Brca2* mutant cells are highly consistent with the notion that HDR is critical for cell reprogramming [17], and they additionally demonstrate that gene complementation not only corrects the reprogramming ability of these cells, but also restores the formation of nuclear Rad51 foci during the reprogramming process. These observations also discard the possibility that accumulated mutations that may have occurred because of the genetic instability of *Brca2*$^{\Delta 27/\Delta 27}$ cells would account for the marked reprogramming defects of these cells. Regarding the causes that limited the reprogramming efficacy of *Brca2*$^{\Delta 27/\Delta 27}$ cells, we demonstrate an increased apoptosis in Brca2$^{\Delta 27/\Delta 27}$ cells during the first stages of cell reprogramming, when a specific DNA damage response—including an activated FA pathway—takes place in the cell [15, 17]. While apparently this contrasts with data from González et al., who did not observe a significant increase in the rate of apoptosis in *Brca2*$^{\Delta 27/\Delta 27}$ with respect to WT cells, these authors analyzed the apoptotic rates in these cells during the expansion of the iPSCs, thus in much later stages of the DNA stress mediated by cell reprogramming.

Our results also show that iPSC clones generated from gene-corrected *Brca2* cells expressed the characteristic pluripotency markers of iPSCs, such as AP, SSEA1, and *Nanog* although did not generate teratomas in NSG animals unless the reprogramming vector was excised from c*Brca2*$^{\Delta 27/\Delta 27}$ iPSCs (Fig. 3 and Supporting Information Fig. S2), consistent with data showing that either the reactivation or the sustained expression of reprogramming transgenes can result in deleterious outcomes such as tumor formation [35] or pluripotency disruption [36].

Significantly, most of our gene complemented *Brca2*$^{\Delta 27/\Delta 27}$ iPSC clones (24 out of 26) became aneuploid at late passages (>17 passages), even though many of them (five out of five) were diploid at passage 4 (Fig. 4C). Moreover, when the reprogramming transgenes were excised from two diploid complemented *Brca2*$^{\Delta 27/\Delta 27}$ iPSC clones, one clone became polyploid, while the other one remained diploid. Even in this clone, aCGH analyses showed the presence of genetic abnormalities that were not detected in their parental *Brca2*$^{\Delta 27/\Delta 27}$ MEFs (Supporting Information Fig. S5). Whether these genetic defects were produced as a direct consequence of c*Brca2*$^{\Delta 27/\Delta 27}$ cell reprogramming or due to the preferential reprogramming or expansion of a reduced population of preexisting abnormal cells, as shown in other experimental models [37–44], remains unknown. Despite the chromosomal changes shown in gene-complemented *Brca2*$^{\Delta 27/\Delta 27}$ iPSC clones, an evident reversion of the FA phenotype was observed in all these clones, as deduced both from the induction of Rad51 foci after MMC treatment and the reduced number of DEB-induced chromosomal abnormalities in corrected versus uncorrected *Brca2*$^{\Delta 27/\Delta 27}$ iPSCs (Fig. 6).

Finally, to evaluate whether gene complemented *Brca2*$^{\Delta 27/\Delta 27}$ iPSCs could be used for the treatment of the hematopoietic defects characteristic of *Brca2*$^{\Delta 27/\Delta 27}$ mice, several differentiation strategies were used. Hematopoietic differentiation c*Brca2*$^{\Delta 27/\Delta 27}$ iPSCs induced by either *Hox-B4* [20, 28, 45, 46] or *Lhx2*-transduction [31] resulted in a population with a modest hematopoietic phenotype, which did not engraft in *Brca2*$^{\Delta 27/\Delta 27}$ recipients. To reconstitute the hematopoietic system of recipient mice with *Fanca*$^{-/-}$ iPS-derived cells, Müller et al. injected gene-corrected *Fanca*$^{-/-}$ iPSCs into WT blastocysts, showing that 1.5% of hematopoietic iPS-derived cells were observed in fetal liver [15]. Although some studies have shown significant hematopoietic engraftments of recipient mice with murine iPSC-derived cells [20, 31], in

other studies only evidences of *in vitro* hematopoietic differentiation were obtained [47]. Significant *in vitro* hematopoietic differentiation has also been observed in human iPSCs from healthy donors [48–50] or patients with monogenic diseases [14, 51, 52], while the *in vivo* repopulating properties of these cells was much more limited.

Conclusion

Our study demonstrates that although *Brca2* mutant cells are defective in cell reprogramming this defect can be overcome by the complementation of their genetic defect, which facilitates the generation of disease-free iPSCs and iPSC-derived hematopoietic cells. Additionally, our results in a HDR relevant model further support the notion that stem cell therapy applications based on combined procedures of gene therapy and cell reprogramming will require further improvements to enhance the genetic stability and the *in vivo* repopulating properties of iPSC-derived cells.

Acknowledgments

We would like to thank Drs. Danwei Huangfu, Christopher Baum, and Jordi Surrallés for helpful discussions; to Sabine Knoess and Johannes Khüle for their collaboration in the experimental work and their contribution with scientific suggestions. We also thank Aurora de la Cal, Sergio Losada, and Angelines Acevedo for their collaboration in the administrative work and Miguel Angel Martín, Jesús Martínez, and Edilia de Almeida for the careful maintenance of the animals. This work was supported by the following grants: European Commission FP7 Program (PERSIST; Ref 222878); Spanish Ministry of Economy and Competitiveness (International Cooperation on Stem Cell Research Plan E; Ref PLE 2009/0100; SAF 2009–07164; and SAF2012–39834), Fondo de Investigaciones Sanitarias, Instituto de Salud Carlos III (RETICS-RD06/0010/0015 and RD12/0019/0023), Dirección General de Investigación de la Comunidad de Madrid (CellCAM; Ref S2010/BMD-2420), and La Fundació Privada La Marató de TV3, 121430/31/32. We also thank the Fundación Marcelino Botín for promoting translational research at the Hematopoietic Innovative Therapies Division of the CIEMAT.

Author Contributions

S.N. and V.M.: conceived and designed the experiments, collection and assembly of data, provision of reagents, materials, analysis tool, ideas, and manuscript writing; JAB: Conceived and designed the experiments, provision of reagents, materials, analysis tool, ideas, and manuscript writing; F.J.M., M.L.L., R.C., E.A., O.Q., T.M., M.G., E.S., U.M., G.G., A.R., and J.C.S.: collection and assembly of data, provision of reagents, materials, analysis tool, and ideas; Y.T.: collection and assembly of data; G.M., N.H., B.S., P.R., and J.C.I.B.: provision of reagents, materials, analysis tool, and ideas. S.N. and V.M. contributed equally to this article.

Disclosure of Potential Conflicts of Interest

The authors indicate no potential conflicts of interest.

References

1 Takahashi K, Yamanaka S. Induction of pluripotent stem cells from mouse embryonic and adult fibroblast cultures by defined factors. Cell 2006;126:663–676.

2 Takahashi K, Tanabe K, Ohnuki M et al. Induction of pluripotent stem cells from adult human fibroblasts by defined factors. Cell 2007;131:861–872.

3 Yu J, Vodyanik MA, Smuga-Otto K et al. Induced pluripotent stem cell lines derived from human somatic cells. Science 2007;318:1917–1920.

4 Stadtfeld M, Nagaya M, Utikal J et al. Induced pluripotent stem cells generated without viral integration. Science 2008;322:945–949.

5 Tiscornia G, Vivas EL, Belmonte JC. Diseases in a dish: Modeling human genetic disorders using induced pluripotent cells. Nat Med 2011;17:1570–1576.

6 Daley GQ. Towards the generation of patient-specific pluripotent stem cells for combined gene and cell therapy of hematologic disorders. Hematology Am Soc Hematol 2007:17–22.

7 Marion RM, Strati K, Li H et al. A p53-mediated DNA damage response limits reprogramming to ensure iPS cell genomic integrity. Nature 2009;460:1149–1153.

8 Li H, Collado M, Villasante A et al. The Ink4/Arf locus is a barrier for iPS cell reprogramming. Nature 2009;460:1136–1139.

9 Utikal J, Polo JM, Stadtfeld M et al. Immortalization eliminates a roadblock during cellular reprogramming into iPS cells. Nature 2009;460:1145–1148.

10 Hong H, Takahashi K, Ichisaka T et al. Suppression of induced pluripotent stem cell generation by the p53-p21 pathway. Nature 2009;460:1132–1135.

11 Banito A, Rashid ST, Acosta JC et al. Senescence impairs successful reprogramming to pluripotent stem cells. Genes Dev 2009;23:2134–2139.

12 Batista LF, Pech MF, Zhong FL et al. Telomere shortening and loss of self-renewal in dyskeratosis congenita induced pluripotent stem cells. Nature 2011;474:399–402.

13 Fong YW, Inouye C, Yamaguchi T et al. A DNA repair complex functions as an Oct4/Sox2 coactivator in embryonic stem cells. Cell 2011;147:120–131.

14 Raya A, Rodriguez-Piza I, Guenechea G et al. Disease-corrected haematopoietic progenitors from Fanconi anaemia induced pluripotent stem cells. Nature 2009;460:53–59.

15 Müller LU, Milsom MD, Harris CE et al. Overcoming reprogramming resistance of Fanconi anemia cells. Blood 2012;119:5449–5457.

16 Yung SK, Tilgner K, Ledran MH et al. Human pluripotent stem cell models of Fanconi anaemia deficiency reveal an important role for Fanconi anaemia proteins in cellular reprogramming and survival of haematopoietic progenitors. Stem Cells 2013;31:1022–1029.

17 González F, Georgieva D, Vanoli F et al. Homologous recombination DNA repair genes play a critical role in reprogramming to a pluripotent state. Cell Rep 2013;3:651–660.

18 Tilgner K, Neganova I, Moreno-Gimeno I et al. A human iPSC model of Ligase IV deficiency reveals an important role for NHEJ-mediated-DSB repair in the survival and genomic stability of induced pluripotent stem cells and emerging haematopoietic progenitors. Cell Death Differ 2013;20:1089–1100.

19 Molina-Estevez FJ, Lozano ML, Navarro S et al. Impaired cell reprogramming in non-homologous end joining deficient cells. Stem Cells 2013;31:1726–1730.

20 Hanna J, Wernig M, Markoulaki S et al. Treatment of sickle cell anemia mouse model with iPS cells generated from autologous skin. Science 2007;318:1920–1923.

21 McAllister KA, Bennett LM, Houle CD et al. Cancer susceptibility of mice with a homozygous deletion in the COOH-terminal domain of the Brca2 gene. Cancer Res 2002;62:990–994.

22 Navarro S, Meza NW, Quintana-Bustamante O et al. Hematopoietic dysfunction in a mouse model for Fanconi anemia group D1. Mol Ther 2006;14:525–535.

23 Cheng NC, van de Vrugt HJ, van der Valk MA et al. Mice with a targeted disruption of the Fanconi anemia homolog Fanca. Hum Mol Genet 2000;9:1805–1811.

24 Raya A, Rodriguez-Piza I, Navarro S et al. A protocol describing the genetic correction of somatic human cells and subsequent generation of iPS cells. Nat Protoc 2010;5:647–660.

25 Rio P, Meza NW, Gonzalez-Murillo A et al. In vivo proliferation advantage of genetically corrected hematopoietic stem cells in a mouse model of Fanconi anemia FA-D1. Blood 2008;112:4853–4861.
26 Sommer CA, Stadtfeld M, Murphy GJ et al. Induced pluripotent stem cell generation using a single lentiviral stem cell cassette. Stem Cells 2009;27:543–549.
27 Charrier S, Ferrand M, Zerbato M et al. Quantification of lentiviral vector copy numbers in individual hematopoietic colony-forming cells shows vector dose-dependent effects on the frequency and level of transduction. Gene Ther 2011;18:479–487.
28 Chan KM, Bonde S, Klump H et al. Hematopoiesis and immunity of HOXB4-transduced embryonic stem cell-derived hematopoietic progenitor cells. Blood 2008; 111:2953–2961.
29 Barrett MT, Scheffer A, Ben-Dor A et al. Comparative genomic hybridization using oligonucleotide microarrays and total genomic DNA. Proc Natl Acad Sci USA 2004;101: 17765–17770.
30 Godthelp BC, Wiegant WW, Waisfisz Q et al. Inducibility of nuclear Rad51 foci after DNA damage distinguishes all Fanconi anemia complementation groups from D1/ BRCA2. Mutat Res 2006;594:39–48.
31 Kitajima K, Minehata K, Sakimura K et al. In vitro generation of HSC-like cells from murine ESCs/iPSCs by enforced expression of LIM-homeobox transcription factor Lhx2. Blood 2011;117:3748–3758.
32 Lesinski DA, Heinz N, Pilat-Carotta S et al. Serum- and stromal cell-free hypoxic generation of embryonic stem cell-derived hematopoietic cells in vitro, capable of multilineage repopulation of immunocompetent mice. Stem Cells Transl Med 2012;1:581–591.
33 Jacome A, Navarro S, Casado JA et al. A simplified approach to improve the efficiency and safety of ex vivo hematopoietic gene therapy in Fanconi anemia patients. Hum Gene Ther 2006;17:245–250.
34 Tulpule A, Lensch MW, Miller JD et al. Knockdown of Fanconi anemia genes in human embryonic stem cells reveals early developmental defects in the hematopoietic lineage. Blood 2010;115:3453–3462.
35 Okita K, Ichisaka T, Yamanaka S. Generation of germline-competent induced pluripotent stem cells. Nature 2007;448:313–317.
36 Niwa H, Miyazaki J, Smith AG. Quantitative expression of Oct-3/4 defines differentiation, dedifferentiation or self-renewal of ES cells. Nat Genet 2000;24:372–376.
37 Mayshar Y, Ben-David U, Lavon N et al. Identification and classification of chromosomal aberrations in human induced pluripotent stem cells. Cell Stem Cell 2010;7:521–531.
38 Hussein SM, Batada NN, Vuoristo S et al. Copy number variation and selection during reprogramming to pluripotency. Nature 2011;471:58–62.
39 Gore A, Li Z, Fung HL et al. Somatic coding mutations in human induced pluripotent stem cells. Nature 2011;471:63–67.
40 Lister R, Pelizzola M, Kida YS et al. Hotspots of aberrant epigenomic reprogramming in human induced pluripotent stem cells. Nature 2011;471:68–73.
41 Laurent LC, Ulitsky I, Slavin I et al. Dynamic changes in the copy number of pluripotency and cell proliferation genes in human ESCs and iPSCs during reprogramming and time in culture. Cell Stem Cell 2011;8: 106–118.
42 Blasco MA, Serrano M, Fernandez-Capetillo O. Genomic instability in iPS: Time for a break. EMBO J 2011;30:991–993.
43 Pasi CE, Dereli-Oz A, Negrini S et al. Genomic instability in induced stem cells. Cell Death Differ 2011;18:745–753.
44 Young MA, Larson DE, Sun CW et al. Background mutations in parental cells account for most of the genetic heterogeneity of induced pluripotent stem cells. Cell Stem Cell 2012;10:570–582.
45 Pilat S, Carotta S, Schiedlmeier B et al. HOXB4 enforces equivalent fates of ES-cell-derived and adult hematopoietic cells. Proc Natl Acad Sci USA 2005;102:12101–12106.
46 Bonde S, Dowden AM, Chan KM et al. HOXB4 but not BMP4 confers self-renewal properties to ES-derived hematopoietic progenitor cells. Transplantation 2008;86:1803–1809.
47 Mukherjee S, Santilli G, Blundell MP et al. Generation of functional neutrophils from a mouse model of X-linked chronic granulomatous disorder using induced pluripotent stem cells. PLoS One 2011;6:e17565.
48 Schenke-Layland K, Rhodes KE, Angelis E et al. Reprogrammed mouse fibroblasts differentiate into cells of the cardiovascular and hematopoietic lineages. Stem Cells 2008;26: 1537–1546.
49 Woods NB, Parker AS, Moraghebi R et al. Brief report: Efficient generation of hematopoietic precursors and progenitors from human pluripotent stem cell lines. Stem Cells 2011;29:1158–1164.
50 Ramos-Mejia V, Montes R, Bueno C et al. Residual expression of the reprogramming factors prevents differentiation of iPSC generated from human fibroblasts and cord blood CD34+ progenitors. PLoS One 2012;7: e35824.
51 Jiang Y, Cowley SA, Siler U et al. Derivation and functional analysis of patient-specific induced pluripotent stem cells as an in vitro model of chronic granulomatous disease. Stem Cells 2012;30:599–611.
52 Xu Y, Liu L, Zhang L et al. Efficient commitment to functional CD34+ progenitor cells from human bone marrow mesenchymal stem-cell-derived induced pluripotent stem cells. PLoS One 2012;7:e34321.


See www.StemCells.com for supporting information available online.